Open Access

Contemporary Research Analysis Journal

e-ISSN: 3050-5909
p-ISSN: 3050-5895

Volume 02 Issue 12 December 2025

CrossRef DOI: 10.55677/CRAJ/02-2025-Vol02I12

Page no: 762-769

Comparison and Characterization of Green Synthesized Silver Oxide Nanoparticles Using *Ziziphus spina-christi* plant extract and AgO NPs by Femtosecond Laser Ablation Technique

Anwar Q. Ahmed[1*], Muthik A. Guda[2]

[1,2] Department of Ecology, Faculty of Science, University of Kufa, Najaf, Iraq

***Corresponding author: Anwar Q. Ahmed**

ABSTRACT: Several techniques have been used, including green manufacturing and femtosecond laser ablation, to synthesize silver oxide nanoparticles (AgO NPs). In this study, low-cost, environmentally friendly green nanomaterials were synthesized and compared to femtosecond laser ablation. Characterization studies demonstrated that the green nanosilver mixture provided a uniform and controlled distribution of silver nanoparticles within the polymer matrix without the addition of any other stabilizers. Transmission electron microscopy (TEM) studies revealed that the size of the green silver nanoparticles was around two times larger than the laser-absorbed method. The interactions between the silver nanoparticles and the mixture were characterized by changes in the intensity of the vibrational peaks and spectral positions. X-ray diffraction (XRD) confirmed the structural modification within the chitosan matrix resulting from the inclusion of silver nanoparticles. Tilt angles were constant for green methods. Absorption changes were studied using ultraviolet-visible (UV-Vis) spectroscopy, and the optical band gap was calculated. The nanosilver exhibits a broad peak at 450 nm, as well as an extract-associated peak at 280 nm, while the silver nanoparticles in the mixture exhibit a broad peak at 427 nm. These results reveal significant differences in the properties of product nanoparticles using the green method and femtosecond laser ablation technique.

KEY WORDS: Z-AgONPs, Silver nanoparticles, femtosecond laser ablation, green synthesized, chitosan

1. INTRODUCTION

Environmentally friendly nanomaterials can be manufactured from natural sources such as bacteria and fungi, but the most important safe source for green nanotechnology is plants, which have proven their efficiency in creating effective and low-cost water treatments, and the resulting sludge is low in biodegradability [1-3]. Silver nanoparticles (AgNPs) are among the most widely materials that are used in research and industry because they possess distinct physical and biological properties compared to pure silver, as evidenced by altered optical and electrical properties. Silver nanoparticles can be used in a variety of applications, such as antibacterial agents [4], electronics, sensors and solar cells [5,6].

Combining polymer composites with nanomaterials is one of the most interesting approaches currently to exploit the common features of polymers and nanomaterials. Chitosan is a natural polymer made from chitin and exhibits excellent properties such as being non-toxic, antimicrobial, biodegradable, and biocompatible with organic compounds [1,4]. Chitin is naturally found in the cell walls of fungi, the exoskeletons of arthropods such as crustaceans and insects, and fish scales [1]. Filling a chitosan matrix with silver nanoparticles holds great potential in medicine, especially in wound dressings and drug delivery due to their antimicrobial properties. The chitosan matrix helps control the release of silver nanoparticles, reducing their toxicity to normal cells [7]. Chitosan materials are used as coating agents to regulate the shape and size of nanoparticles and to stabilize the synthesized silver nanomaterials [8-11].This study aims to compare the green synthesis of AgONPs from (Leaves of *Ziziphus spina-christi* plants extracts) and the fabrication of a new chitosan-blend composite film filled with concentrated silver nanoparticles (laser-ablated), using a simple method for their production and to study their physical properties. This in-depth study also discusses the optical and structural properties of both methods using different techniques.

2. MATERIALS AND METHODS

Treatment of plant

Z. spina-christi Leaves were collected and attended as stated in the literature of (Al Bayati *et al*., 2020).

$AgNO_3$ Solution Preparation and (AgNPs) A Green Synthesis

To create a usable 1 mM silver nitrate solution, 0.016987 gram of silver nitrate was dissolved in 100 ml of deionized water. (AgNPs) of the *Z. spina-christi* extract were produced using the procedure described in the literature of [12], which involved mixing 10 ml of the extract. Preliminary evidence of the formation of AgNPs was obtained by watering the plant with 100 ml of a 1 mM con. of silver nitrate solution, heating the mixture on a magnetic vibrating plate at 45 C° for 20 minutes, and observing the mixture's color change. The weights were prepared for every 1 ml of sterile distilled water, and the amount was preserved until used in the various experiments.

Preparation of Chitosan (AgNPs) Synthesis

Chitosan (from Fluka, USA) were utilized as a blend matrix for filling with AgNPs (synthesized by femtosecond laser ablation method); the distilled water was used as solvent.

Chitosan was prepared by dissolving it in distilled water containing 2% acetic acid. These components were then mixed to form a mixture of 20 wt.% chitosan. Silver nanoparticles (AgNPs) were combined in distilled water with the polymer blend in pre-calculated amounts under the same conditions to obtain silver nano composite samples in the concentration of 19.8 ml.280 ppm/w. The solution was then placed in Petri dishes at 45 °C for approximately 48 h. After complete drying, the nanocomposite films were separated from the Petri dishes and stored in vacuum desiccators until use.

Physical characteristics of AgNPs

Using a French scanning electron microscope $MIRA_3$ FTM, the prepared samples were examined to determine the size and shape of the particles [13]. Approximately 5 microliters of the ready-to-examine solutions were placed on an electron microscope holder made of carbon and gold, and the sample was left to dry at room temperature before being examined under various magnifications. The prepared AgNPs' size and diameter, as well as their surface morphology and roughness, were studied by using an atomic force microscope (Angstrom Advanced AA2000). To prepare for testing, a tiny drop of the sample solution was put on a 1 × 1 cm glass slide and allowed to dry at room temperature [14]. X-ray diffraction spectroscopy was used to measure the phase variation and grain size of AgNPs [15]. 48 hours after the green nanoparticles were prepared, a sample was obtained and subjected to a UV spectrometer examination at 190–1100 nanometers in wavelength. The water used was distilled deionized. At room temperature, the product's optical characteristics were evaluated [16].

Statistical analysis

Data was analyzed by (ANOVA) method and (LSD) Test.

3. RESULTS AND DISCUSSION

3.1 Characterization of silver nanoparticles

3.1.1 Transmission electron microscopy (TEM)

Transmission electron microscopy (TEM) was used to measure the size of the produced silver nanoparticles. Figure (1) shows TEM images of pure green silver nanoparticles and AgONPs removed by laser in aqueous solution. It reveals that the green nanoparticles were approximately spherical in shape, randomly distributed, with diameters ranging from 50 to 70 nm. The laser-removed ones appeared as even, well-packed cubes, with diameters ranging from 30 to 60 nm. Figure (3) due to the aggregation that occurred as a result of the presence of cell components on the surface of the nanoparticles, as it served as a barrier agent. This agrees with that was obtained in [17], who observed the morphology and composition of silver nanoparticles using extracts of the *Tridux procumbens* plant, also [17] stated that the silver nanoparticles extracted from cinnamon and sage plants were characterised with spherical as shown in figure (1).

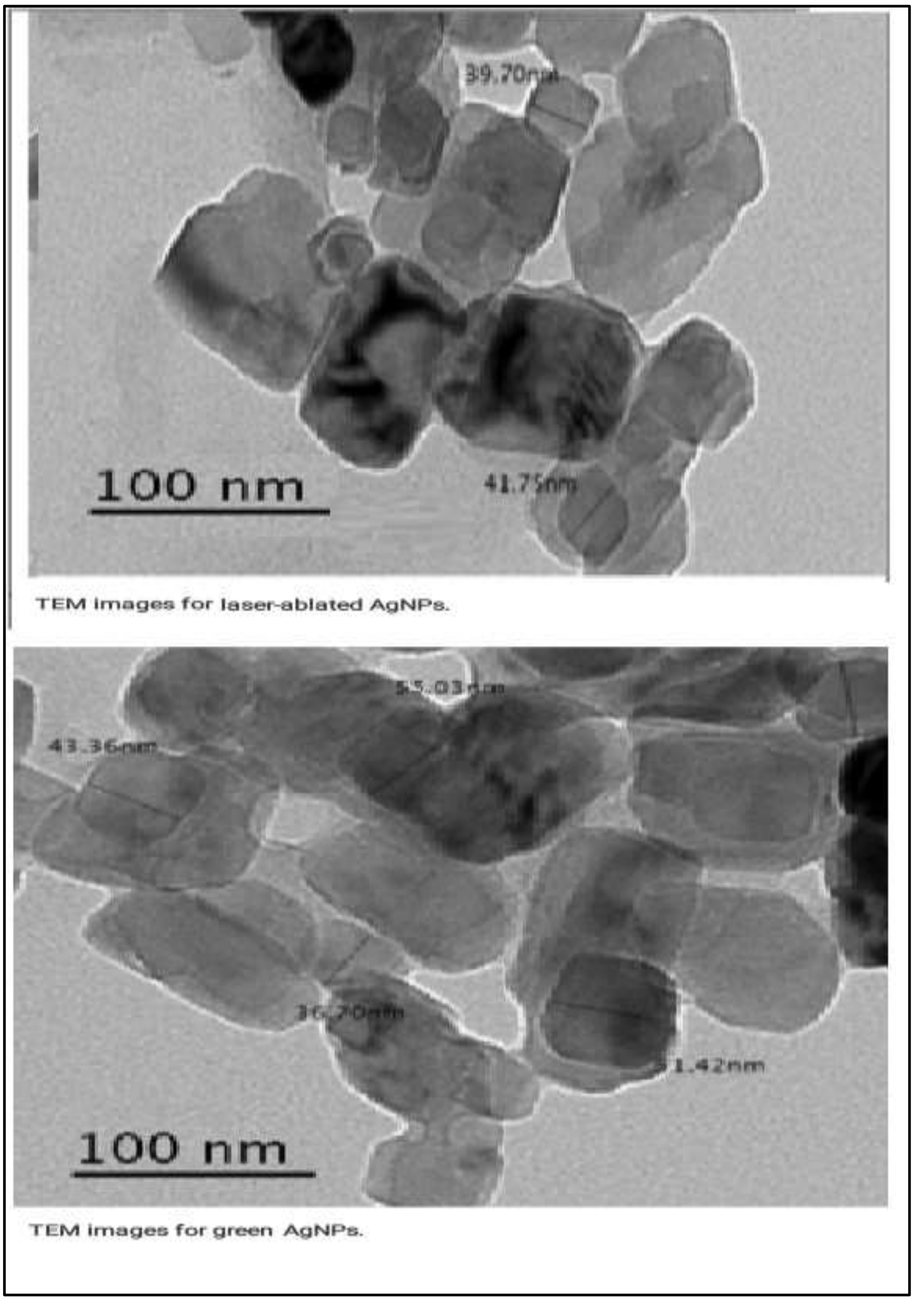

Figure 1. TEM images for green and laser ablated AgO NPs

3.1.2. X-Ray Diffractometer (XRD)

Figure (2) shows a green manufacturing by reducing Ag+ ions using buckthorn extract is crystalline in nature, and all peaks that observed in the XRD pattern can easily be classified as having a structure of central cubic structure. The average size of the nanocrystals was estimated by using the Scherrer equation:

$$D = 0.9\lambda / \beta \cos\theta \qquad (1)$$

where the average size of the crystals according to the measurement was 24.37 nm. This also agreed with results of [18], in the preparation of silver nanoparticles using a water extract from some plant leaves, and the silver nanoparticles showed clear peaks.

Figure (3) shows the X-ray diffraction (XRD) of chitosan filled with a concentration of silver nanoparticles (AgNPs) in the diffraction angle extending from 3° to 70°. Filling the mixture with silver nanoparticles also reduces the intensity of the peak at $2\theta = 19.4°$, which depends on the interaction between the filler and the mixture, which reduces the intermolecular interaction between the mixture chains, and works to lower the degree of crystallinity [19]. This amorphous nature is responsible for the high ionic diffusion, which leads to a higher ionic conductivity [20]. This behavior indicates that the chitosan matrix has undergone a structural modification as a result of the filling of silver nanoparticles and confirms the results that were obtained in the FTIR studies. Furthermore, it can be observed from the same figure that after filling with a high content of extracted silver nanoparticles, a new peak is generated at ~38°, which can be attributed to the face-centered cubic (fcc) structure of the embedded silver nanoparticles, which corresponds to the parameters h k l (111) [21].

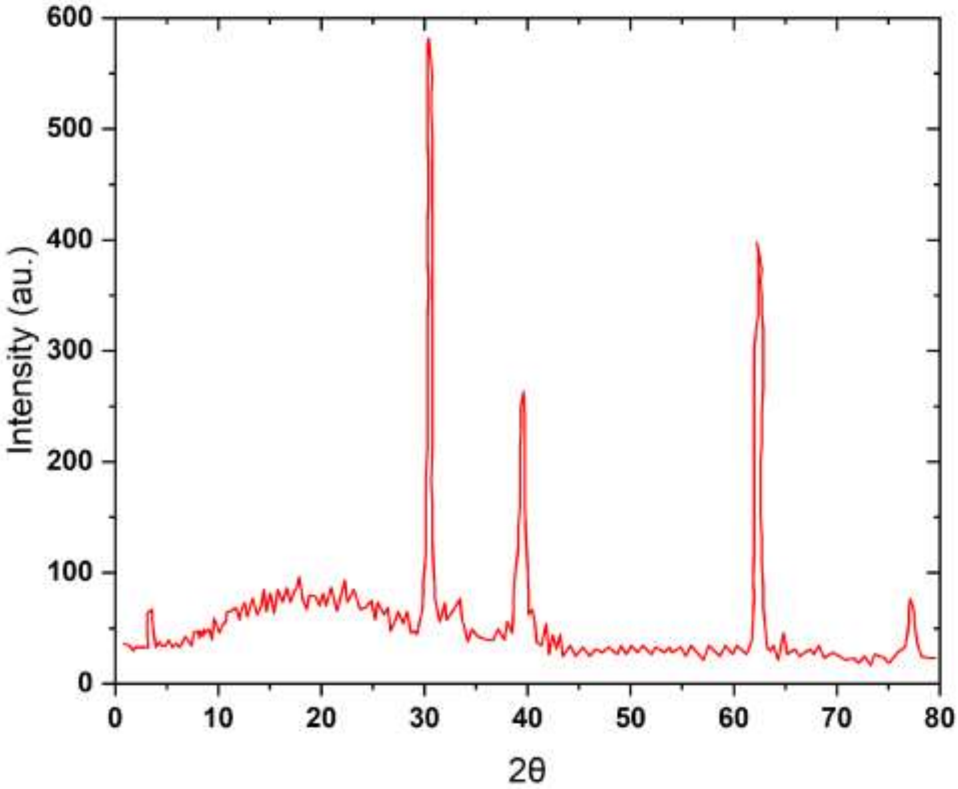

Figure 2. X-ray diffraction (XRD) of AgNPs from the buckthorn plant

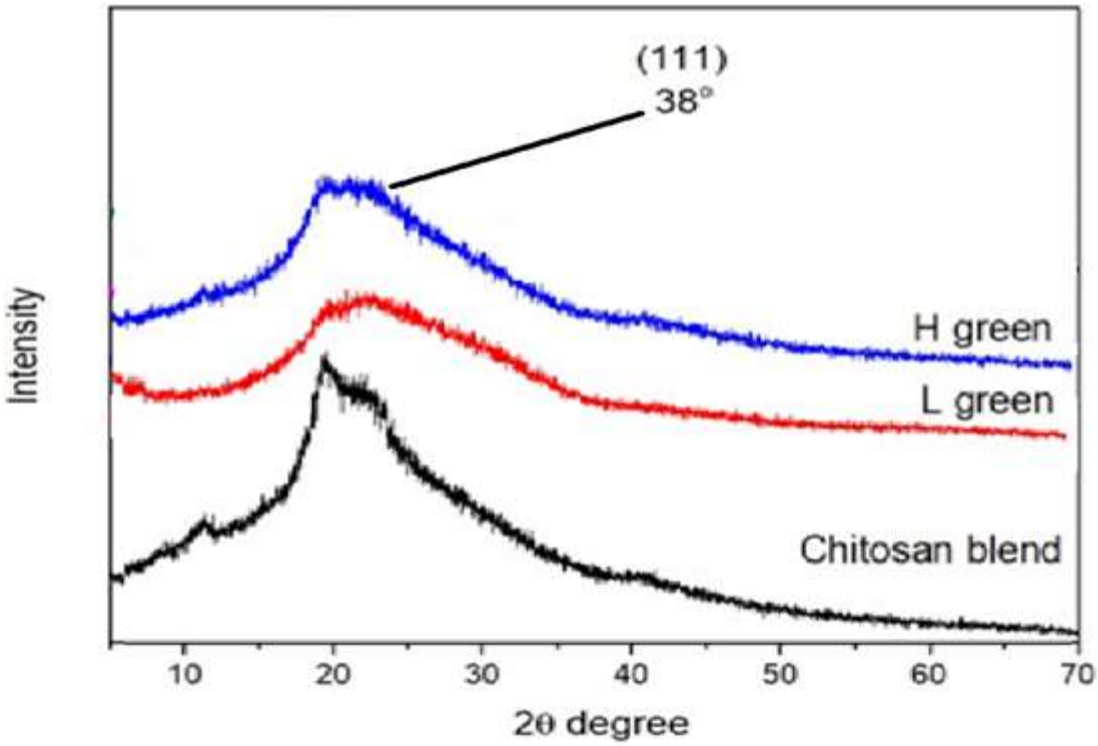

Figure 3. X-ray diffraction (XRD) of chitosan pure and filled chitosan blend with AgNPs

3.1.3. UV/VIS absorption and optical studies

Figure (4) shows the UV/Vis absorption spectra of the chitosan nanocomposite samples. The absorbance values at a wavelength of 200 nm can be attributed to the interaction between the polymer matrix and the added silver nanoparticles, which affects the calculated optical band gap [22] associated with the crystallinity change in the nanocomposites. In addition, a peak begins to appear at λmax = 427 nm, and its intensity increases continuously with increasing silver nanoparticle concentration. The appearance of this peak in the visible range is attributed to the surface plasmon resonance (SPR) nature of the silver nanoparticles incorporated in an insulating medium, which results from the collective excitation of the conduction band electrons in the nanoparticle. The presence of these peaks also indicates that the synthesized mixture can be used as a good cross-linking agent for silver nanoparticles. The increase in λmax (and hence the decrease in the optical band gap energy) means that the particle size increases with increasing filler concentration [23], indicating that the laser-exfoliated silver nanoparticles have a larger size than those obtained from green-coated silver nanoparticles.

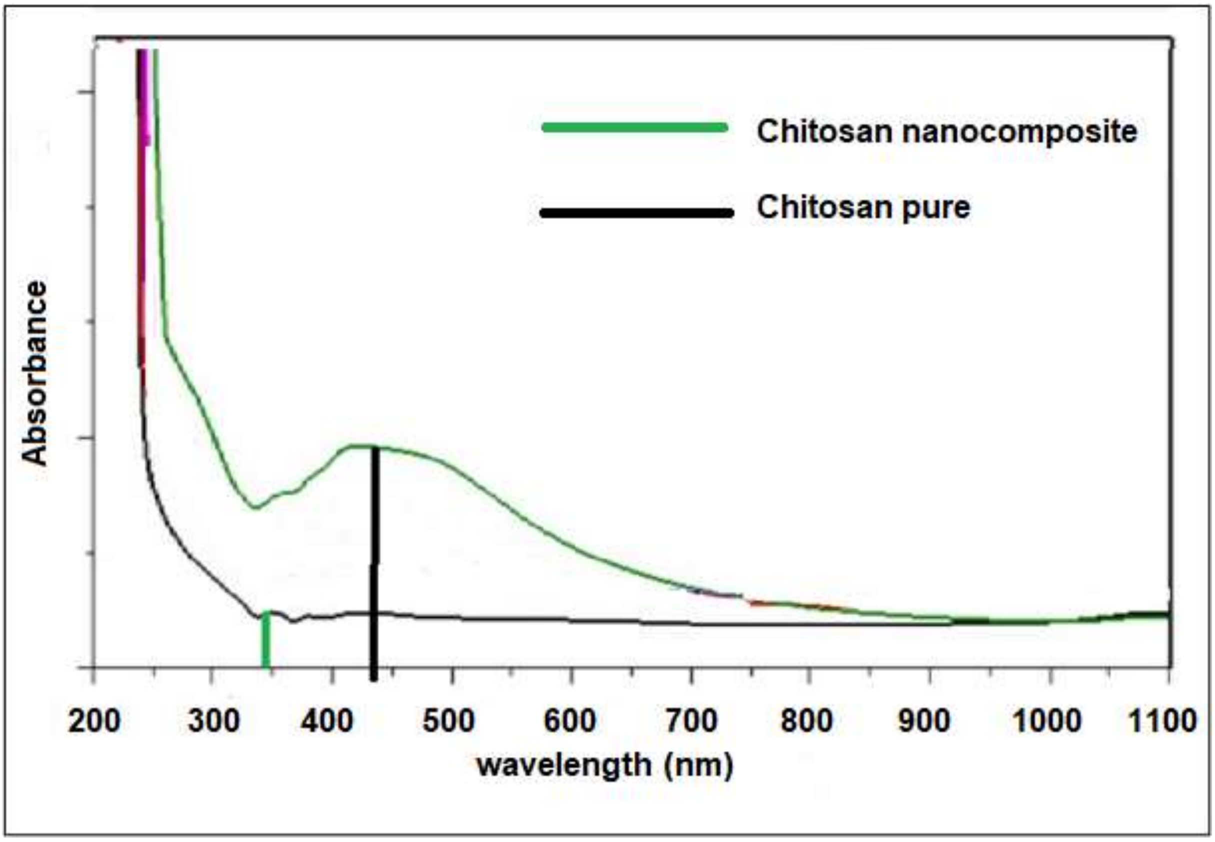

Figure 4. UV/VIS absorption spectra of the chitosan pure and nanocomposite samples

Figure 5.a. shows the highest absorption peak for the crude extract at a wavelength of 228 nm. While figure 5.b. showed the presence of silver nanoparticles, as the absorption peak was recorded at a wavelength of 440 nm. This result is within the diagnostic limits for silver nanoparticles, which range between 400 and 450 nm, due to surface plasmon absorption. This phenomenon occurs as a result of the dipole oscillation that is formed when the electromagnetic field within the visible range is coupled with the collective oscillation of conduction electrons. The plasmon resonance phenomenon often occurs for metallic surfaces of silver and gold when a light beam is directed and strikes the metallic surface at a specific angle and depends on the thickness of the molecular layer of the metal surface. Therefore, the size of the formed particles can be counted within the size limits of nanomaterials [24]. This result is consistent with the study of [25,26], as the UV-visible spectrometer for examining silver nanoparticles manufactured from ivy and aloe vera extracts showed that the highest absorption peak was at wavelengths of 419-427 respectively. The results of the current study are also consistent with those of [27]. The results of examining silver nanoparticles manufactured from celery and myrtle extracts using UV-visible spectroscopy showed the highest absorption peak at wavelengths 408-410 respectively, which are within the absorption range of silver metal, which ranges from 400 nm to 450-

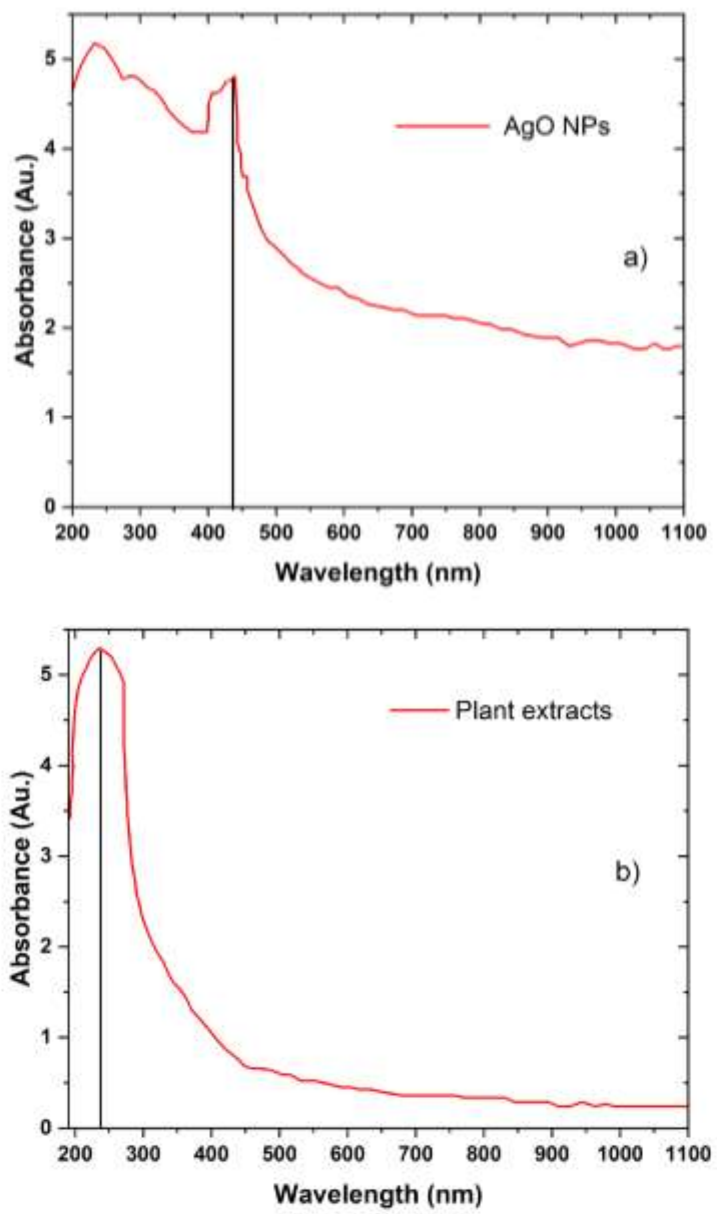

Figure 5. UV/VIS absorption spectra of the Z-AgONPs and plant extracts samples

4. CONCLUSION

Silver oxide nanoparticles were synthesized by green methods using an aqueous extract of sea buckthorn. A chitosan mixture filled with silver nanoparticles was prepared using a common casting technique. Transmission electron microscopy (TEM) investigations confirmed the presence of Z-AgONPs with diameters ranging from 50 to 70 nm, while in the case of chitosan, silver nanoparticles of diameters ranging from 30 to 65 nm were produced. X-ray analysis showed that Z-AgONPs have a spherical crystalline shape, while chitosan, after filling with highly corrosive silver nanoparticles, generates a peak at 38 °C. This can be attributed to the face-centered cubic (fcc) structure of the embedded silver nanoparticles, which corresponds to the h k l (111) parameters. UV/Visible and Fourier transform infrared spectroscopy data revealed that Z-AgONPs possess more than just strong activity, due to the interaction of the active compounds in the plant extract and the formation of complexes with the prepared polymers and/or silver nanoparticles. This can be observed in the UV band expansion and redshift, which can be attributed to intermolecular interactions between hydrogen bonds. The study results showed that the optical band gaps are significantly reduced by filling, as filling with silver nanoparticles which produce levels of charge-carrier-rich traps. All these data support the idea that green nanofabrication produces stable and efficient silver nanocomposites, compared to complex formation between silver nanoparticles and a blended matrix.

Author Contributions: Conceptualization, A.Q.A.; methodology, M. A. G.; validation, A. Q. A. investigation, M. A. G.; writing—original draft preparation, M. A. G. and H. A. A.; writing—review and editing, A.Q.A. and M. A. G.

Funding Information: This work was funded by A.Q.A. and M. A. G.

Conflicts of Interest: The authors declare no conflict of interest.

Data Availability Statement: The raw and processed data required to reproduce these results are available by reasonable request.

Acknowledgements
This work was supported by the Department of Ecological Science, faculty of science, Kufa university

Conflicts of Interest: The authors declare no conflict of interest.

REFERENCES

1. Guda, M. A., Nasir, A. S., Younus, A. S., & Altamimi, A. J. (2018). Antioxidant enzyme responses of Juncus Aschers.(Et Buch.) Adams to some of environmental stresses and use it as indicators. indian journal of public health research & development, 9(12), 1102-1107.
2. Al Bayati, F.S., Al Naqeeb, N.A., Guda, M.A., Almansoori, D.H.H. (2020). Use of phytoplankton enzyme in the artificial lake as indicator of pollution , Journal of Chemical Health Risks, 10(4), pp. 353–359
3. Kumar, A., Dutt, D., & Kumar, V. (2019). Groundwater quality assessment in river Hindon catchment of Saharanpur, Uttar Pradesh, India. International Journal of Agricultural & Statistical Sciences, 15(1).
4. Garibo, D., Borbón-Nuñez, H. A., de León, J. N. D., García Mendoza, E., Estrada, I., Toledano-Magaña, Y., ... & Susarrey-Arce, A. (2020). Green synthesis of silver nanoparticles using Lysiloma acapulcensis exhibit high-antimicrobial activity. Scientific reports, 10(1), 12805.
5. Sreeja, S., Prabhakaran, S., & Pesala, B. (2020). Efficiency enhancement of betanin dye-sensitized solar cells using plasmon-enhanced silver nanoparticles. In Advances in Energy Research, Vol. 1: Selected Papers from ICAER 2017 (pp. 9-18). Springer Singapore.
6. Algburi, J. B., Saheb, L., Anwar, Q. A., & Almayahi, B. A. (2018). UV-VIS and SEM Assessment of Silver Nanoparticles Synthesized using Nd-YAG Laser as antibacterial. Research Journal of Pharmacy and Technology, 11(4), 1588-1591.
7. Al-Shamari, A. A., Abdelghany, A. M., Alnattar, H., & Oraby, A. H. (2021). Structural and optical properties of PEO/CMC polymer blend modified with gold nanoparticles synthesized by laser ablation in water. Journal of Materials Research and Technology, 12, 1597-1605.
8. Guda, M. A., Hakeem, J. I., Alabassi, M. M., and Almayahi, B. A. (2017). Effects of Environmental Stress on Nutrients of Typha domingensis Pers. Plant in Najaf, Iraq. Annual Research and Review in Biology, 1-6.
9. Algethami, N., Rajeh, A., Ragab, H. M., Tarabiah, A. E., & Gami, F. (2022). Characterization, optical, and electrical properties of chitosan/polyacrylamide blend doped silver nanoparticles. Journal of Materials Science: Materials in Electronics, 33(13), 10645-10656.
10. Varma, R., & Vasudevan, S. (2020). Extraction, characterization, and antimicrobial activity of chitosan from horse mussel modiolus modiolus. ACS omega, 5(32), 20224-20230.
11. Luo, S., Qiao, X., Wang, Q. Y., Zhang, Y. F., Fu, P., Lin, Z. D., ... & Cheng, C. (2019). Excellent self-healing and antifogging coatings based on polyvinyl alcohol/hydrolyzed poly (styrene-co-maleic anhydride). Journal of Materials Science, 54(7), 5961-5970.
12. Alabassi, M. M., Guda, M. A., & Muhammed, M. A. (2022). The removal efficiency of natural nano-coagulant produced from Phragmites communis, Schanginia aegyptiaca and Portulaca oleracea in wastewater treatment. International Journal of Aquatic Biology, 10(2), 181-186.
13. Mukherji, S., Bharti, S., Shukla, G., & Mukherji, S. (2019). Synthesis and characterization of size-and shape-controlled silver nanoparticles. Physical Sciences Reviews, 4(1), 20170082.
14. Husayn, D. M., & Guda, M. A. (2023, July). Response of some wild plants in antioxidant enzymes by zinc oxide nanoparticles. In AIP Conference Proceedings (Vol. 2787, No. 1). AIP Publishing.
15. Ali, M. H., Azad, M. A. K., Khan, K. A., Rahman, M. O., Chakma, U., & Kumer, A. (2023). Analysis of crystallographic structures and properties of silver nanoparticles synthesized using PKL extract and nanoscale characterization techniques. ACS omega, 8(31), 28133-28142.
16. Owied, O. A. R., Guda, M. A. M., Taher, H. I., & Abdulhussein, M. A. A. (2021). Plants Anatomical Engineered By Nanomaterials. Revis Bionatura 2023; 8 (2) 44. Iranian Journal of Ichthyology.
17. Husayn, D. M., & Guda, M. A. (2023, July). Effect of zinc oxide nanoparticles on biomarkers of chlorophyll and carotene in some wild plants. In AIP Conference Proceedings (Vol. 2787, No. 1). AIP Publishing.

18. Menazea, A. A., Ismail, A. M., Awwad, N. S., & Ibrahium, H. A. (2020). Physical characterization and antibacterial activity of PVA/Chitosan matrix doped by selenium nanoparticles prepared via one-pot laser ablation route. Journal of Materials Research and Technology, 9(5), 9598-9606.
19. Abdelghany, A. M., Menazea, A. A., & Ismail, A. M. (2019). Synthesis, characterization and antimicrobial activity of Chitosan/Polyvinyl Alcohol blend doped with Hibiscus Sabdariffa L. extract. Journal of Molecular Structure, 1197, 603-609.
20. Sharma, V., Verma, D., & Okram, G. S. (2020). Influence of surfactant, particle size and dispersion medium on surface plasmon resonance of silver nanoparticles. Journal of Physics: Condensed Matter, 32(14), 145302.
21. Abdelrazek, E. M., Abdelghany, A. M., Badr, S. I., & Morsi, M. A. (2018). Structural, optical, morphological and thermal properties of PEO/PVP blend containing different concentrations of biosynthesized Au nanoparticles. Journal of materials research and technology, 7(4), 419-431.
22. Saravanan, R., Aviles, J., Gracia, F., Mosquera, E., & Gupta, V. K. (2018). Crystallinity and lowering band gap induced visible light photocatalytic activity of TiO2/CS (Chitosan) nanocomposites. International journal of biological macromolecules, 109, 1239-1245.
23. Venkatachalam, S. (2016). Ultraviolet and visible spectroscopy studies of nanofillers and their polymer nanocomposites. Spectroscopy of polymer nanocomposites, 130-157.
24. Morin-Crini, N., Lichtfouse, E., Torri, G., & Crini, G. (2019). Applications of chitosan in food, pharmaceuticals, medicine, cosmetics, agriculture, textiles, pulp and paper, biotechnology, and environmental chemistry. Environmental Chemistry Letters, 17(4), 1667-1692.
25. Gami, F., Algethami, N., Ragab, H. M., & Tarabiah, A. E. (2022). Structural, optical and electrical studies of chitosan/polyacrylamide blend filled with synthesized selenium nanoparticles. Journal of Molecular Structure, 1257, 132631.
26. Algethami, N., Rajeh, A., Ragab, H. M., Tarabiah, A. E., & Gami, F. (2022). Characterization, optical, and electrical properties of chitosan/polyacrylamide blend doped silver nanoparticles. Journal of Materials Science: Materials in Electronics, 33(13), 10645-10656.
27. Kurakula, M., & Rao, G. K. (2020). Pharmaceutical assessment of polyvinylpyrrolidone (PVP): As excipient from conventional to controlled delivery systems with a spotlight on COVID-19 inhibition. Journal of drug delivery science and technology, 60, 102046.